Supplemental Data

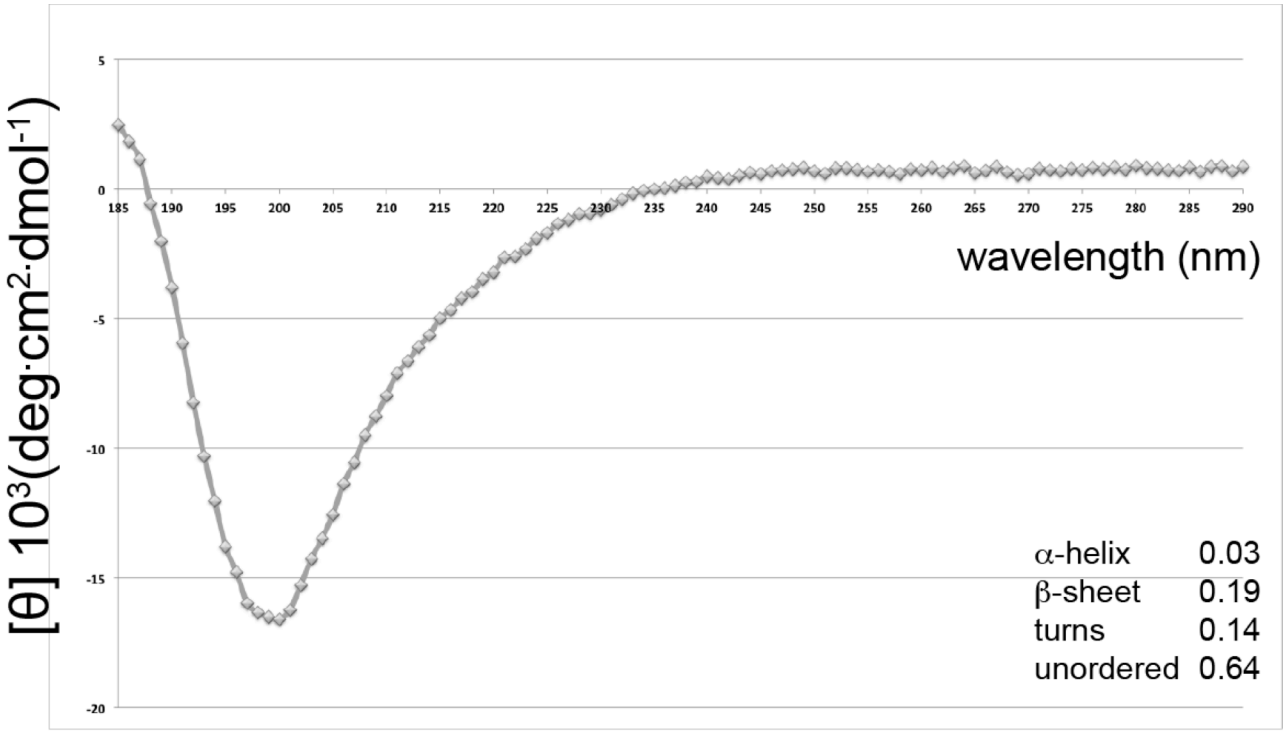

Fig. S1

Figure S1, related to Figure 2C. Secondary structure analysis of KyoT2. Figure shows far-UV spectroscopy (wavelengths 185-200nm) for KyoT2 (184-210). The CD spectrum has a distinct minimum at 200 nm, characteristic of random coil. Relative amounts of secondary-structure were determined from CD data using Dichroweb and CDSSTR with reference set 7. The normalized root mean square deviation parameter value for analysis of the KyoT2 CD data is 0.012.

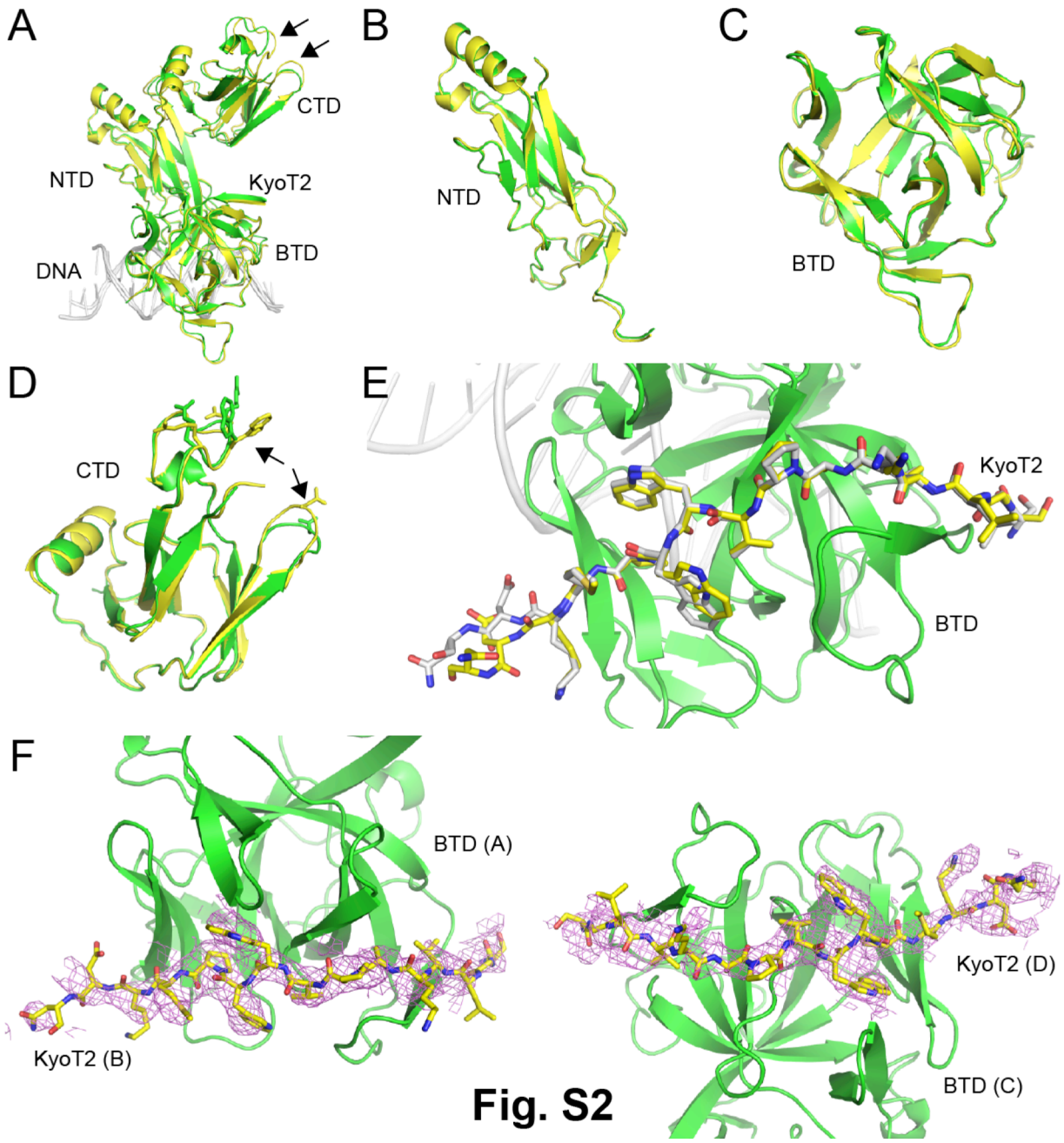

Fig. S2

Figure S2, related to Figure 3. Structural alignment of the two CSL-KyoT2-DNA complexes contained within the asymmetric unit. Figure shows structural overlay of the two CSL-KyoT2-DNA complexes within the asymmetric unit (AU). (A) Corresponding cα atoms from the two CSL molecules contained within the AU were aligned, exhibiting an overall 0.66 RMSD. (B) Corresponding cα atoms from the NTD from the two CSL molecules contained within the AU were aligned, exhibiting a 0.27 RMSD. (C) Corresponding cα atoms from the BTD from the two CSL molecules contained within the AU were aligned, exhibiting a 0.23 RMSD. (D) Corresponding cα atoms from the CTD from the two CSL molecules contained within the AU were aligned, exhibiting a 0.31 RMSD. (E) Corresponding cα atoms from the two KyoT2 molecules contained within the AU were aligned, exhibiting a 0.24 RMSD. (F) Figure shows 2Fo-Fc density, contoured at 1σ, from molecular replacement solution (prior to refinement) for KyoT2 with final refined model. Protein chains are denoted in parentheses.Arrows (panels A & D) indicate structural differences in the CTD between the two complexes within the AU.

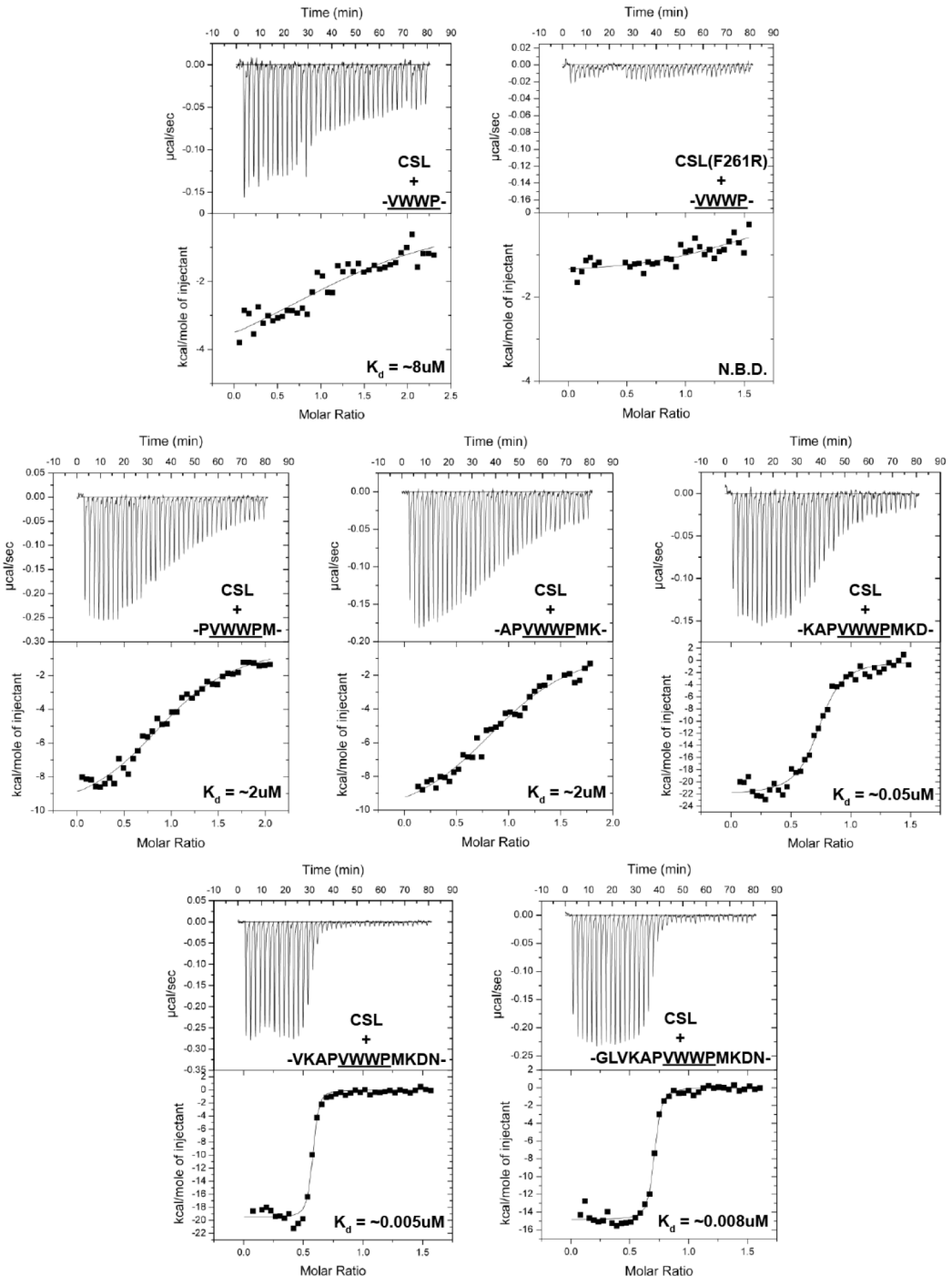

Figure S3, related to Figure 4. Identification of the minimal KyoT2 peptide that specifically binds CSL. This figure shows representative thermograms (raw heat signal and nonlinear least squares fit to the integrated data) for wild-type and mutant (F261R) CSL binding to KyoT2 peptides of decreasing lengths. KyoT2 peptide sequences and apparent dissociation constants are denoted on each thermogram. The hydrophobic tetrapeptide motif (-VWWP-) is underlined. Complete thermodynamic binding data is shown in Table S2. NBD=no binding detected.

Table S1, related to Figure 4F. Buried surface area comparison of CSL-KyoT2 and CSL-RAM complex structures.

Complex	Organism	PDB ID	Total BSA (Å^2)	Nonpolar BSA (Å^2)	Ratio (NP/Total)
CSL – KyoT2	Mouse	4J2X	874	602	0.7
CSL – RAM	Worm	3BRD	950	654	0.7
CSL – NICD – MAM	Worm	2FO1	904	536	0.6
CSL – NICD – MAM	Human	3V79	930	647	0.7

Table S2, related to Table 2. Calorimetric binding analysis of KyoT2 residues required for minimal binding to CSL.

CSL	KyoT2 Ligand	K_{app} (M^{-1})	K_d (uM)	ΔG_{obs} (kcal/mol)	ΔH_{obs} (kcal/mol)	$-T\Delta S_{obs}$ (kcal/mol)
WT	-VWWP-	1.2 ± 0.6 x 10^5	8.3	-6.9	-5.0 ± 1.0	-1.9 ± 0.5
F261R	-VWWP-	*NBD*	---	---	---	---
WT	-PVWWPM-	4.6 ± 0.7 x 10^5	2.2	-7.7	-10.4 ± 0.4	2.7 ± 0.3
WT	-APVWWPMK-	5.7 ± 1.0 x 10^5	1.8	-7.9	-10.8 ± 0.5	3.0 ± 0.5
WT	-KAPVWWPMKD-	2.1 ± 0.4 x 10^7	0.048	-10.0	-22.2 ± 0.4	12.2 ± 0.5
WT	-VKAPVWWPMKDN-	1.8 ± 0.5 x 10^8	0.006	-11.2	-19.1 ± 0.2	7.9 ± 0.9
WT	-GLVKAPVWWPMKDN-	1.2 ± 0.3 x 10^8	0.008	-11.0	-14.8 ± 0.1	3.8 ± 0.6

All experiments were performed at 25°C. The errors represent the standard deviation of the nonlinear least squares fit of the data to the titration curves. NBD=No Binding Detected.

Table S3, related to Table 4. Comparison of KyoT2, RAM, and EBNA2 ITC binding data to CSL

CSL mutant	Ligand	K_d (uM)	~fold difference
WT	KyoT2	0.012	---
WT	RAM (N1)	0.022	---
WT	RAM (N2)	0.032	---
WT	EBNA2	4.6	---
F261R	KyoT2	6.3	525
F261R	RAM (N1)	15	682
F261R	RAM (N2)	9.5	297
V263R	KyoT2	0.019	1.6
V263R	RAM (N1)	0.43	20
V263R	RAM (N2)	3.6	113
A284R	KyoT2	7.2	600
A284R	RAM (N1)	0.74	34
A284R	RAM (N2)	2.5	78
Q333R	KyoT2	0.051	4.3
Q333R	RAM (N1)	0.38	17
Q333R	RAM (N2)	0.20	6.3

ITC binding data for the RAM domains from Notch1 (N1) and Notch2 (N2) were taken from Yuan, Z., Friedmann, D. R., Vanderwielen, B. D., Collins, K. J., & Kovall, R. A. (2012). Characterization of CSL (CBF-1, Su(H), Lag-1) mutants reveals differences in signaling mediated by Notch1 and Notch2. *The Journal of biological chemistry*, *287*(42), 34904–34916. The ITC binding data for EBNA2 were taken from Johnson, S. E., Ilagan, M. X. G., Kopan, R., & Barrick, D. (2010). Thermodynamic analysis of the CSL x Notch interaction: distribution of binding energy of the Notch RAM region to the CSL beta-trefoil domain and the mode of competition with the viral transactivator EBNA2. *The Journal of biological chemistry*, *285*(9), 6681–6692.